

Antiferromagnetic resonance in the cubic perovskite KNiF_3

H. Yamaguchi, K. Katsumata, M. Hagiwara, and M. Tokunaga
The Institute of Physical and Chemical Research (RIKEN), Wako, Saitama 351-0198, Japan

H. L. Liu,* A. Zibold, and D. B. Tanner
Department of Physics, University of Florida, Gainesville, Florida 32611

Y. J. Wang
National High Magnetic Field Laboratory, Tallahassee, Florida 32306
 (Received 9 September 1998)

Low-temperature high-magnetic-field far-infrared spectroscopy and electron-spin-resonance measurements have been performed on single crystals of the cubic perovskite KNiF_3 . We found the absorption at $48.7 \pm 0.3 \text{ cm}^{-1}$ observed by Richards [P. L. Richards, J. Appl. Phys. **34**, 1237 (1963)] that was attributed to antiferromagnetic resonance (AFMR) is not magnetic in origin. Instead, a different absorption is well fit by a theory of AFMR with uniaxial anisotropy. Analysis yields an anisotropy energy of $8.7 \times 10^{-3} \text{ cm}^{-1}$. The ratio between the anisotropy field and the exchange field is 2.4×10^{-5} . Thus, KNiF_3 is an excellent example of a Heisenberg antiferromagnet. [S0163-1829(99)00209-X]

Perovskite materials have received enormous attention in the past decade, largely because both high-temperature superconductors and colossal magnetoresistance materials are based on perovskite structures. In this paper, we revisit the prototypical cubic perovskite KNiF_3 , the best known example of a Heisenberg antiferromagnet, and report both the far-infrared spectrum in high magnetic fields and the electron-spin-resonance (ESR) spectrum.

The crystal structure of KNiF_3 is an ideal perovskite type and it retains its room-temperature symmetry down to 78 K.¹ Heat-capacity measurements^{2,3} showed an anomaly at 253 K (Ref. 2) or at 253.5 K,³ indicating an occurrence of magnetic ordering. The magnetic susceptibility² of this compound also displayed a fairly broad peak at 275 K. The magnetic structure of KNiF_3 was confirmed by neutron-diffraction measurements,⁴ which showed that the magnetic moment is coupled antiferromagnetically to its six nearest neighbors, i.e., G type. In the antiferromagnetic phase, the spins point parallel to [100] (or equivalently, [010] or [001]) observed by magnetic torque measurements.⁵

Theoretically, Lines⁶ studied the magnetic properties of KNiF_3 and described them in terms of an isotropic spin Hamiltonian,

$$\mathcal{H} = \sum_{\langle i,j \rangle} J \vec{S}_i \cdot \vec{S}_j - \sum_i [g \mu_B S_{iz} H_z + 4 \mu_B^2 H_z^2 / \Delta], \quad (1)$$

where J is the nearest-neighbor exchange interaction constant, \vec{S} is the spin operator ($|\vec{S}| = 1$), g is the g value, μ_B is the Bohr magneton, H_z is the external magnetic field parallel to the z axis, and Δ is the energy difference between the ground and first excited orbital levels. From an analysis of the magnetic susceptibility, $J = 89 \pm 4 \text{ K}$ was obtained. More recently, an *ab initio* calculation⁷ gave $J = 81 \text{ K}$ in reasonable agreement with the results reported by Lines.⁶

The magnetic excitation spectrum of KNiF_3 below the Néel temperature (T_N) was studied by far-infrared

spectroscopy.⁸ An absorption at $48.7 \pm 0.3 \text{ cm}^{-1}$ was observed well below T_N and was attributed to an antiferromagnetic resonance (AFMR). If one were to fit this absorption using a standard theory of AFMR,⁹ the value of the anisotropy energy would be about 3.2 cm^{-1} . This value is, however, incompatible with other experiments, which show that KNiF_3 is an ideally isotropic antiferromagnet.

In order to obtain information about the magnetic anisotropy, we have performed far-infrared spectroscopy and ESR measurements on single crystals of KNiF_3 . It turns out that the absorption reported by Richards⁸ is not magnetic in origin. Our results show an absorption line, which is well fit by the theory of AFMR with very small uniaxial anisotropy. Additionally, we observe several weak lines at low fields in the ESR measurements.

The single crystals of KNiF_3 used in this study were grown by a flux method. The typical dimensions are $5 \times 2.5 \times 0.5 \text{ mm}^3$. The far-infrared absorption measurement in zero field was performed using a Bruker IFS-120HR Fourier-transform spectrometer installed in RIKEN. This spectrometer covers the frequency range from 10 to 4000 cm^{-1} with a resolution of about 0.002 cm^{-1} . The temperature of the sample was varied between 4.2 and 300 K by using a continuous-flow helium cryostat (Oxford Instruments CF1104). Far-infrared studies in a magnetic field were measured at the National High Magnetic Field Laboratory in Tallahassee. These measurements used a Bruker IFS-113V spectrometer and light-pipe optics to carry the unpolarized far-infrared radiation through the 30 T resistive magnet. The propagation direction was parallel to the static magnetic field. We report the field-dependent transmittance ratio at the constant temperatures running over a range between 4.2 and 40 K. The ESR measurement was performed using a high-frequency high-field spectrometer. A detailed description of the ESR set up is given elsewhere.^{10,11}

Figure 1 shows the far-infrared spectra of KNiF_3 taken in zero field at various temperatures. At 4.2 K, we see a strong

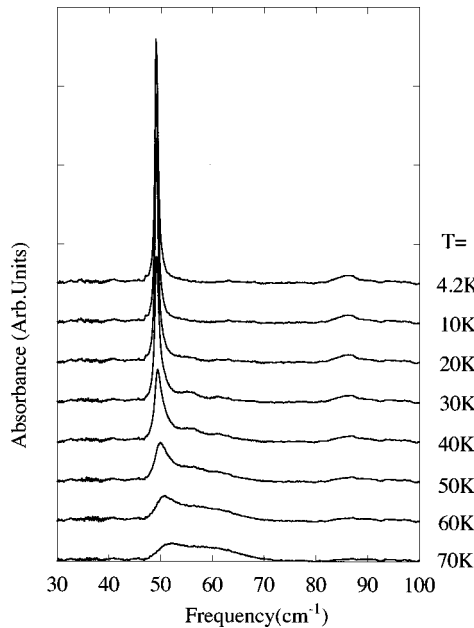


FIG. 1. Temperature dependence of the far-infrared spectra of KNiF_3 in zero field. The curves have been offset for clarity.

absorption near 49 cm^{-1} and a weaker one around 86 cm^{-1} . Additionally, a very weak absorption is observed at $\sim 94 \text{ cm}^{-1}$. The frequency of the strong absorption is in good agreement with that reported by Richards.⁸ Interestingly, the intensity and line shape of 49 cm^{-1} resonance are a strong function of temperature. The oscillator strength of this peak decreases systematically with increasing temperature and the high-energy sideband mode gradually grows in intensity. The 4.2 K far-infrared results in magnetic fields are shown in the inset of Fig. 2. The energy of three low-frequency modes is nearly independent of a magnetic field up to 30 T, indicating these absorptions are not magnetic in origin.

In addition to these field-independent features, we observe an absorption whose frequency does depend on the magnetic

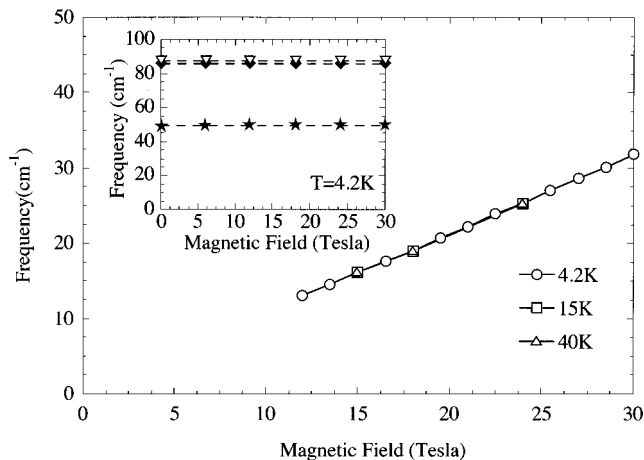


FIG. 2. An absorption mode in KNiF_3 measured at various fields and temperatures. The inset shows magnetic-field dependence of three low-frequency absorptions in KNiF_3 at 4.2 K. The external magnetic field is applied parallel to the $[100]$ direction.

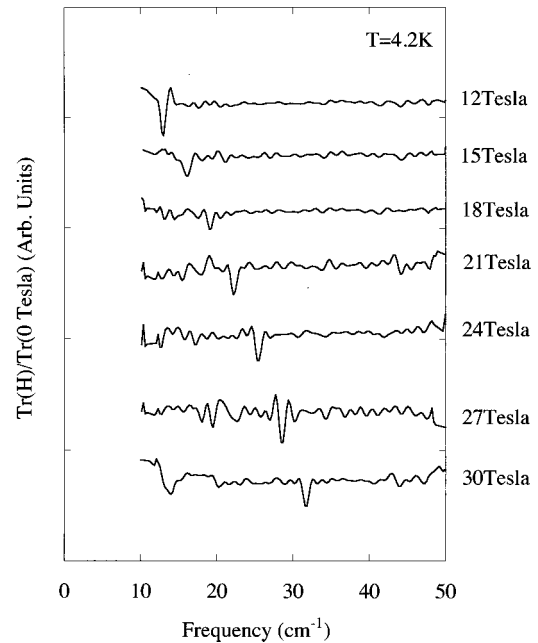


FIG. 3. Far-infrared transmission ratio spectra of KNiF_3 at 4.2 K at applied magnetic fields up to 30 T. The spectra taken at finite fields are normalized by one at zero field. The curves have been offset for clarity.

field. Figure 3 shows the far-infrared spectra taken at 4.2 K and at various fields. The data were obtained by taking the ratio of the transmission of the sample at a given field to the zero-field transmission. We plot in Fig. 2 the frequency of the absorption as a function of magnetic field. Notably, the peak position of this absorption increases almost linearly with applied magnetic field. Furthermore, the field-dependent behavior of this absorption does not change with temperatures between 4.2 and 40 K.

Because the low-frequency limit of the far-infrared spectrometer is about 10 cm^{-1} , we made ESR measurements of KNiF_3 below 340 GHz (11.3 cm^{-1}). The inset of Fig. 4

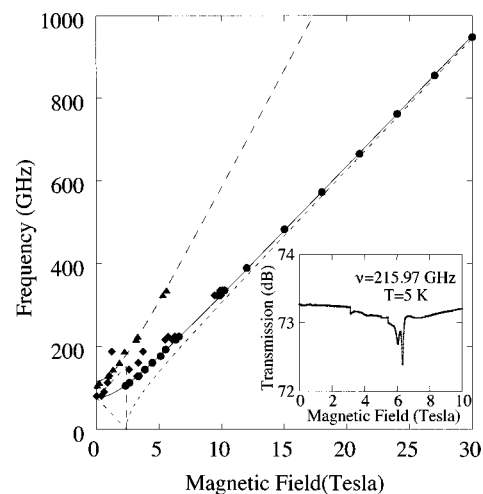


FIG. 4. Absorption frequencies versus magnetic field (symbols) for KNiF_3 from both the far-infrared ($T = 4.2 \text{ K}$) and ESR ($T = 5 \text{ K}$) measurements. Full, dotted, and dashed lines are the theoretical fits described in the text. The inset shows the 5 K ESR spectrum of KNiF_3 taken at a frequency of 215.97 GHz.

displays the ESR data taken at the frequency of 215.97 GHz ($\sim 7.2 \text{ cm}^{-1}$). There are three absorptions in the spectrum. A strong absorption is seen at 6.35 T, a weaker one at 6.07 T, and a very weak one at 3.18 T.

We summarize in Fig. 4 all the field-dependent absorptions of KNiF_3 observed by far-infrared and ESR measurements; these absorptions constitute a magnetic excitation branch in the frequency-magnetic-field plane. We analyze this branch using the theory of AFMR (Ref. 9) with uniaxial anisotropy. When the external magnetic field H is applied parallel to the easy axis, the AFMR frequency ν at low temperatures ($T \ll T_N$) is given by

$$2\pi\nu/\gamma = \sqrt{2H_E H_A \pm H}, \quad (H < H_{\text{SF}}) \quad (2)$$

and

$$2\pi\nu/\gamma = \sqrt{H^2 - 2H_E H_A}, \quad (H > H_{\text{SF}}), \quad (3)$$

where $\gamma (= g\mu_B/\hbar)$ is the magnetomechanical ratio, H_E is the exchange field, H_A is the anisotropy field, and H_{SF} is the spin-flop field. When H is applied perpendicular to the easy axis, the AFMR frequency is given by

$$2\pi\nu/\gamma = \sqrt{2H_E H_A + H^2}. \quad (4)$$

The full line in Fig. 4 is the fit to our data using Eq. (4) with $(\gamma/2\pi)\sqrt{2H_E H_A} = 76.1 \text{ GHz} (= 2.54 \text{ cm}^{-1})$ and $g = 2.26$. The g value obtained in this fit is close to that determined from earlier ESR measurements¹² of $\text{KMgF}_3:\text{Ni}^{2+}$ ($g = 2.28$). Using the value of $J = 89 \text{ K} (= 62 \text{ cm}^{-1})$ derived by Lines,⁶ we obtain $g\mu_B H_E = 370 \text{ cm}^{-1}$ at low temperatures ($T \ll T_N$), where the thermal average of Ni spin is 1. Then, using the experimental value of $(\gamma/2\pi)\sqrt{2H_E H_A} = 76.1 \text{ GHz}$, we estimate $g\mu_B H_A = 8.7 \times 10^{-3} \text{ cm}^{-1}$.

This anisotropy energy is too small to be accounted for either by the magnetic dipole-dipole interaction (typically of the order of 0.1 cm^{-1}) or by a single-ion anisotropy of the form DS_z^2 (typically of the order of 1 cm^{-1}). Thus, consistent with the results of x-ray diffraction,¹ we conclude that the cubic symmetry is retained below T_N . We also notice that Money *et al.*,¹³ found a small tetragonal distortion below T_N by a double-crystal x-ray-diffraction and strain gauge measurements. They interpreted this distortion as due to magnetostriction. The magnetostriction constant is so small ($\lambda_{100} \sim 10^{-5}$) at 77 K that the anisotropic energy would be

also very small. The ratio between H_A and H_E in KNiF_3 is 2.4×10^{-5} . Thus, KNiF_3 is an excellent example of a Heisenberg antiferromagnet.

It is important to mention that the AFMR modes predicted by Eqs. (2) and (3) are not observed in our data. As first pointed out by Hirakawa and co-workers⁵ and later observed by x-ray synchrotron topography,¹⁴ three domains dx , dy , and dz exist in zero field for the cubic antiferromagnet. The easy axes of the dx , dy , and dz domains point parallel to the $[100]$, $[010]$, and $[001]$ crystallographic axes, respectively. When the external magnetic field is applied parallel to one of the cube axes, for example, $[001]$, the dx and dy domains grow at the expense of the dz domains. This occurs because χ_{\perp} is larger than χ_{\parallel} (χ_{\parallel} and χ_{\perp} are the magnetic susceptibility parallel and perpendicular to the easy axis, respectively). This domain growth is associated with a movement of domain walls. From the x-ray topography,¹⁴ the domain-wall movement occurs in the field range between 0.22 and 0.45 T. Therefore, only the magnetic domains whose easy axis is perpendicular to the external field are relevant to our study.

Finally, we briefly discuss the weak absorptions observed in the ESR experiments. The weak absorption near the main signal in the inset of Fig. 4 may be an interference fringe. We try to fit the weak absorption observed at 3.18 T (see Fig. 4) to the AFMR theory. The dashed line in Fig. 4 represents the fit [Eq. (4)] with $g = 4.09$ and $(\gamma/2\pi)\sqrt{2H_E H_A} = 115.8 \text{ GHz}$. One possible explanation for this excitation would be that it originates from a nonlinear excitation. Further studies are necessary to clarify this point.

In conclusion, we have made far-infrared and ESR measurements on single crystals of KNiF_3 . We observe an AFMR mode. An analysis of this AFMR mode gives a very small anisotropy energy ($8.7 \times 10^{-3} \text{ cm}^{-1}$) and confirms that KNiF_3 is the best example of a Heisenberg antiferromagnet.

This work was partially supported by the ‘‘MR Science Research Program’’ from RIKEN. H.L.L., A.Z., and D.B.T. acknowledge support from the NHMFL and the NHMFL In-House Research Program under NSF Contract No. DMR-952703. The work performed at the National High Magnetic Field Laboratory in Tallahassee is supported by NSF Cooperative Agreement No. DMR-9527035 and by the state of Florida.

*Present address: Frederick Seitz Materials Research Laboratory, University of Illinois at Urbana-Champaign, Urbana, Illinois 61801.

¹A. Okazaki and Y. Suemune, J. Phys. Soc. Jpn. **16**, 671 (1961).

²K. Hirakawa, K. Hirakawa, and T. Hashimoto, J. Phys. Soc. Jpn. **15**, 2063 (1960).

³C. Deenadas, H. V. Keer, R. V. G. Rao, and A. B. Biswas, Indian J. Pure Appl. Phys. **5**, 147 (1967).

⁴V. Scatturin, L. Corliss, N. Elliott, and J. Hastings, Acta Crystallogr. **14**, 19 (1961).

⁵K. Hirakawa, T. Hashimoto, and K. Hirakawa, J. Phys. Soc. Jpn. **16**, 1934 (1961).

⁶M. E. Lines, Phys. Rev. **164**, 736 (1967).

⁷R. L. Martin and F. Illas, Phys. Rev. Lett. **79**, 1539 (1997).

⁸P. L. Richards, J. Appl. Phys. **34**, 1237 (1963).

⁹T. Nagamiya, K. Yosida, and R. Kubo, Adv. Phys. **4**, 1 (1955).

¹⁰M. Hagiwara, K. Katsumata, I. Yamada, and H. Suzuki, J. Phys.: Condens. Matter **8**, 7349 (1996).

¹¹M. Hagiwara, K. Katsumata, H. Yamaguchi, M. Tokunaga, I. Yamada, M. Gross, and P. Goy (unpublished).

¹²K. Knox, R. G. Shulman, and S. Sugano, Phys. Rev. **130**, 512 (1963).

¹³D. G. Money, D. M. Paige, W. D. Corner, and B. K. Tanner, J. Magn. Magn. Mater. **15-18**, 603 (1980).

¹⁴M. Safa and B. K. Tanner, Philos. Mag. B **37**, 739 (1978).